JOURNAL OF AGRICULTURAL AND FOOD CHEMISTRY

Article

pubs.acs.org/JAFC

Resveratrol Nanoparticle System Improves Dissolution Properties and Enhances the Hepatoprotective Effect of Resveratrol through Antioxidant and Anti-Inflammatory Pathways

Chiang-Wen Lee,[†] Feng-Lin Yen,[‡] Haw-Wei Huang,[§] Tzu-Hui Wu,[⊥] Horng-Huey Ko,[‡] Wen-Sheng Tzeng,*[,#] and Chun-Ching Lin*[,§,∥]

[†]Department of Nursing, Division of Basic Medical Sciences, and Chronic Diseases and Health Promotion Research Center, Chang Gung University of Science and Technology, Chia-Yi, Taiwan

[‡]Department of Fragrance and Cosmetic Science, [§]Graduate Institute of Natural Products, and [∥]School of Pharmacy, College of Pharmacy, Kaohsiung Medical University, Kaohsiung, Taiwan

[⊥]Health Bureau of Kaohsiung County Government, Kaohsiung, Taiwan

[#]Chi-Mei Foundation Hospital, Tainan, Taiwan

ABSTRACT: Resveratrol (RES), a well-known antioxidant and anti-inflammatory compound, is abundant in red wine and exerts numerous pharmacological effects, including hepatoprotection and cadioprotection. Unfortunately, RES is restricted in clinical application due to poor dissolution property and adsorption. In addition, red wine as a supplement for preventing disease is not recommended for patients with alcohol-related disorders. To address these limitations, we successfully developed a novel RES nanoparticle system (RESN) and demonstrated that RESN could circumvent the physicochemical drawbacks of raw RES with respect to dissolution, such as the reduction of particle size, amorphous transformation, and hydrogen-bond formation. In addition, we employed an animal model of CCl_4-induced hepatotoxicity to estimate the potential of the nanoparticle formulation to improve the hepatoprotective effect of orally administered RES. Our results demonstrated that RESN can diminish liver function markers (aspartate aminotransferase and alanine aminotransferase) by decreasing hepatocyte death due to CCl_4-induced hepatotoxicity in rats, when compared with RES administration. The effect was achieved by reducing oxidative stress (decreased reactive oxygen species and lipid peroxidation) and lowering inflammatory cytokines (decreased tumor necrosis factor-α and interleukin 1β) and protein expression (cyclooxygenase-2, inducible nitric oxide synthase, cytosolic phospholipase A2, and caspase-3). In conclusion, enhancement of the dissolution of RES through a nanoparticle engineering process can result in increased hepatoprotective effects mediated by antioxidant and anti-inflammatory activities. Consequently, we suggest that RESN deserves further study, perhaps in prophylaxis of chronic liver diseases.

KEYWORDS: *resveratrol, nanoparticles, hepatoprotective, antioxidant, anti-inflammatory*

INTRODUCTION

In the human body, many drugs and toxic chemicals are metabolized by the liver and converted to nontoxic substances. Oxidative stress and severe inflammatory response are the major mechanisms of hepatotoxicity, although harmful toxic chemicals can directly injure the liver.[1] An external supply of antioxidants is essential to suppress the inflammation response and for defense against the deleterious effects of oxidative stress.[2]

Dietary polyphenols, such as resveratrol (RES), could be effectively used to prevent aggravation in many diseases by virtue of their antioxidant activities.[3] It is well-known that red wine is one of the most commonly consumed alcoholic beverages and one of the richest sources of RES in the human diet.[4] Consumption levels of up to 300 mL daily can provide enough RES to prevent cardiovascular diseases,[5] but excessive consumption is harmful to patients with alcohol-related disorders such as alcoholic hepatitis and gastrointestinal tract disease.[6,7] However, the poor water solubility of RES is the major limiting factor in preclinical dissolution testing for drug and health food applications.

RES is one of the major active antioxidants in red wine and blueberries.[4,8] Previous studies have demonstrated that RES exerts many pharmacological effects, including antioxidant, anti-inflammatory, anticancer, neuroprotective, cardioprotective, and hepatoprotective effects.[9−14] RES has considerable potential to be developed into a daily supplement, but there are still two problems to be solved before it can be found in clinical application: poor water solubility and high costs.[15] Over the past few decades, the application of delivery systems has been used to improve the dissolution and bioavailability of poorly water-soluble compounds.[16] In the pharmaceutical industry, a dissolution study of a poorly water-soluble drug is usually performed before the determination of bioavailability in a clinical trial.[17] Hu et al. have reported that nanoparticle engineering processes (NPS) are excellent drug delivery systems for the enhancement of the dissolution percentage of

Received: December 6, 2011
Revised: March 25, 2012
Accepted: April 5, 2012
Published: April 5, 2012

poorly water-soluble drugs; such processes include nanoprecipitation, wet milling, and high-pressure homogenization.[18]

Our aim was to use Eudragit E100 (EE100) and polyvinyl alcohol (PVA) as excipients to prepare a RES nanoparticle system (RESN) by a nanoparticle engineering process. We determined particle size, amorphous transformation, and hydrogen-bonding formation to elucidate the mechanism of enhancement of dissolution percentage of RESN. Additionally, we investigated the antioxidant and anti-inflammatory mechanism for elucidating the hepatoprotective effect of RESN, and compared these outcomes with those obtained with free RES to confirm the pharmacological effect.

MATERIALS AND METHODS

Chemicals. RES, PVA, Tris-HCl, thiobarbituric acid (TBA), sodium dodecyl sulfate (SDS), acetic acid, and 2′,7′-dichlorodihydrofluorescein diacetate (H2DCF-DA) were purchased from Sigma-Aldrich Chemicals Co. (St. Louis, MO). Potassium dihydrogen phosphate (KH_2PO_4) was purchased from Mallinckrodt Baker, Inc. (Phillipsburg, NJ). EE100 (aminoalkyl methacrylate copolymers) was kindly provided by Röhm Pharma (Dramstadt, Germany). All other chemical regents were of analytical grade.

Preparation of Resveratrol Nanoparticle Formulation and Physical Mixture. The RESN was prepared using the modified nanoprecipitation technique as described previously and the advantages of the method are its simplicity, quickness, and low cost.[19] RESN preparation used inexpensive apparatus, such as a homogenizer and rotary vacuum evaporator, and it only involved three simple steps, including drug dissolving, homogenization, and solvent evaporation, and the period needed for RESN preparation is less than 1 h. EE100 and PVA were used as excipients to prepare the resveratrol nanoparticle formulation by nanoprecipitation with the solvent-evaporation method. PVA (400 mg) was dissolved with stirring in 150 mL of distilled−deionized water. EE100 (400 mg) was dissolved in 50 mL of 95% ethanol in an ultrasonic water bath. RES (100 mg) was added to this organic solution until it dissolved. The organic solution was then rapidly injected with a 20 mL syringe into the aqueous solution, and the solution was mixed with a homogenizer at 22 000 rpm for 25 min. The mixed solution was subjected to rotary vacuum evaporation in a 40 °C water bath to remove residual ethanol. An aliquot (100 mL) of the remaining solution, RESN, was stored in a refrigerator for use in hepatoprotective effect assays. The lyophilized powder of RESN was collected with a freeze-dryer and stored in a moisture-proof container before physicochemical characterization. In addition, we mixed 100 mg of RES, 400 mg of EE100, and 400 mg of PVA to prepare the physical mixture with a mortar for comparison of physicochemical characteristics of RESN.

Physicochemical Characterization of RES and RESN. Determination of physicochemical characteristics of different samples was performed as described by Wu et al.[20] The particle size and polydispersity index of RES and RESN were determined by photon correlation spectroscopy with a N5 submicrometer particle size analyzer (Beckman Coulter). For determination of amorphous transformation, RES, resveratrol physical mixture (RESPM), RESN, and nanoparticle without resveratrol (BN) were examined by differential scanning calorimetry (DSC, Perkin-Elmer, Norwalk, CT) and X-ray diffractometry (XRD, Siemens D5000). Hydrogen-bond formation between RES and excipients was determined by Fourier transform infrared spectroscopy (FTIR, Perkin-Elmer, Norwalk, CT) and ^{1}H nuclear magnetic resonance (^{1}H NMR, Oxford Instrument Co., Abingdon, Oxfordshire, UK). All measurements were performed in triplicate.

Determination of Encapsulation Efficiency and Yield of RESN. The encapsulation efficiency and yield of RESN were determined by measuring the amount of RES encapsulated with the nanoparticle formulation. Briefly, the RES standard curve was performed by high-performance liquid chromatography (HPLC, Hitachi). The HPLC analysis system was composed of Hitachi interface D-7000 module, pump (L-7100), autosampler (L-7200), and UV−vis detector (L-7420). The chromatographic separation was performed using LichroCART 250-4 Purospher STAR RP-18e (250 × 4.6 mm i.d., 5 μm). The mobile phase was composed of 25 mM potassium dihydrogen phosphate buffer and acetonitrile (50:50, v/v). Different RES concentrations (1−100 μg/mL) were eluted at a flow rate of 1 mL/min, and retention time was detected by a UV−vis detector at 290 nm. The resulting calibration curve of RES was linear (r^2 = 0.999) and was used to calculate the encapsulation efficiency and yield. The amount of RES encapsulated within RESN and its yield were determined by the method of Yen et al. using eqs 1 and 2.[12]

$$\text{encapsulation efficiency (\%)} = \frac{\text{RESN encapsulation} - \text{RESN unencapsulation}}{\text{RESN encapsulation}} \times 100 \quad (1)$$

$$\text{yield (\%)} = \frac{\text{actual amount of RES in RESN}}{\text{theoretical amount of RES in RESN}} \quad (2)$$

Determination of Dissolution Percentage of RES and RESN. The dissolution percentage of the RES and RESN were determined using the dissolution paddle method of USP XXIV in a dissolution apparatus (SR8Plus, Hanson Virtual Instrument, Chatsworth, CA). RES and RESN were added to 100 mL of hydrochloride buffer solution (pH 1.2) and acetate buffer solution (pH 4.5) to simulate the gastric and small intestine according to USP XXIV. The samples were stirred with a rotating paddle at 100 rpm. Sample collection times were set at 5, 10, 20, 40, 60, 90, and 120 min, at which time 1 mL of each sample was filtered through a 0.45-μm filter (Millex-HV Millipore). The RES concentration of all samples was analyzed by HPLC procedures as described above.

Determination of in Vivo Hepatoprotective Activity. Male Wistar rats were purchased from BioLasco Taiwan Co. Ltd. All rats received humane care, and the experimental protocol was approved by the Animal Research Committee of Kaohsiung Medical University of Taiwan. Rats were housed in animal cages and fed standard rodent chow and water ad libitum. Animals were acclimatized to the controlled environment following the Animal Use Protocol of Kaohsiung Medical University for 1 week. Experimental analysis of carbon tetrachloride (CCl_4) induced acute hepatotoxicity was performed according to the method of Ikeda et al. with some modifications.[21] Rats weighting 180−200 g were randomized into four groups of five rats in each group. Group 1 (vehicle group) rats were gavaged with distilled water for 3 days. Group 2 (vehicle + CCl_4) rats were gavaged with nanoparticles without RES for 3 days. Groups 3 and 4 (experimental groups) were treated with 20 mg/kg RES dissolved in water and 20 mg/kg RESN for 3 days, respectively. On day 4, group 1 was treated with olive oil (2.5 mL/kg), and all other groups were treated with a single dose of 20% CCl_4 in olive oil (2.5 mL/kg) by intraperitoneal injection. After 24 h, all rats were sacrificed and blood was collected by cardiac puncture with a sterilized syringe. Blood samples were centrifuged at 3000 rpm for 10 min to separate the serum. For determination of liver function, the aspartate aminotransferase (AST) and alanine aminotransferase (ALT) levels of the serum were determined using an autoanalyzer (Hitachi 7050, Tokyo, Japan). The histopathological observations of the liver tissues of all groups were estimated using hematoxylin and eosin staining, and then observed for the histopathological changes of liver injury by photomicroscope. In addition, we used commercial ELISA kits for tumor necrosis factor-α (TNF-α) and interleukin 1β (IL-1β) (Quantikine, R&D Systems, Minneapolis, MN) to determine serum levels of inflammatory cytokines.

Determination of Antioxidant Activities. Liver tissue was homogenized with 150 mM Tris-HCl buffer (pH 7.2) to prepare a 20% (w/v) liver homogenate. The content of reactive oxygen species (ROS) in liver tissue was determined using the modified method of Llacuna et al.[22] Briefly, 20 μL of liver homogenate was added to 980 μL of phosphate-buffered saline. An aliquot (950 μL) of this solution was mixed with 50 μL of 100 μM H2DCF-DA, and samples were

incubated in a 96-well microplate for 30 min at room temperature in the dark. Absorbance was measured by a fluorescence reader (FLx 800, Bio-Tek Instruments Inc., Winooski, VT) at an excitation wavelength of 485 nm and emission wavelength of 530 nm. All measurements were performed in triplicate.

In addition, the antilipid peroxidation was determined by using the modified method of Ohkawa et al.[23] Briefly, homogenate (40 μL) was placed into a 2-mL microtube and then mixed with the following in order: 40 μL of 9.8% SDS, 300 μL of 20% acetic acid, 300 μL of 0.8% TBA, and 120 μL of distilled−deionized water. The samples were heated at 95 °C for 1 h and immediately placed in an ice−water bath to cool down to room temperature. Samples were then mixed with 1 mL of *n*-butanol and centrifuged at 3000 rpm for 10 min. Supernatants were analyzed by measuring the absorbance at 532 nm. All determinations were performed in triplicate.

Analysis of Inflammatory Protein Expression by Western Blot. Liver samples were lysed in radioimmunoprecipitation assay (RIPA) buffer containing 50 mM Tris−HCl (pH 7.4), 150 mM NaCl, 1% NP-40, 0.5% sodium deoxycholate, 0.1% SDS, 2 mM phenylmethylsulfonyl fluoride, 1 mM sodium orthovanadate, and 2 g/mL each of aprotinin, leupeptin, and pepstatin. After 10 min of centrifugation at 15 000 rpm, 4 °C, volumes equivalent to 50 μg of protein were denatured and subjected to SDS−PAGE using a 12% running gel and then transferred to nitrocellulose membranes. Membranes were incubated with anti-cyclooxygenase-2 (COX2), anti-cytosolic phospholipase A2 (cPLA2), anti-inducible nitric oxide synthase (iNOS), anti-caspase 3 (Santa Cruz Biotechnology, Santa Cruz, CA), and anti-GAPDH (Enzo Life Sciences, Plymouth Meeting, PA) antibodies for 24 h, and then membranes were incubated with anti-mouse or anti-rabbit horseradish peroxidase antibody for 1 h. The immunoreactive bands detected by ECL reagents were developed by Hyperfilm-ECL. All determinations were performed in triplicate.

Statistical Analysis. All data are expressed as mean value ± standard deviation. All mean values were analyzed using one-way analysis of variance (ANOVA) followed by a posthoc test of LSD (SPSS 13, Chicago, IL). $P < 0.05$ was considered statistically significant.

RESULTS

The Reduction of Particle Size. As shown in Table 1, the particle sizes of raw RES and RESN were 11 172.9 ± 3120 and 73.8 ± 1.14 nm, respectively. These results indicate that EE100 and PVA had effectively minimized the particle size of RES using a simple nanoprecipitation. In addition, the polydispersity index (PI) of PCS analysis is effectively used to determine the particle distribution of any particle system. The distribution of particle size broadens when the PI value is greater than or equal to 1 and displays a narrow distribution when the PI value is less than or equal to 0.3. Our results show that RESN (PI = 0.16 ± 0.01) displayed the uniform particle distribution of RES (PI = 1.11 ± 0.19).

Table 1. Particle Size, Polydispersity, Yield and Encapsulation Efficiency of the Resveratrol Nanoparticle Formulation[a]

	particle size (nm)	polydispersity	yield (%)	encapsulation efficiency (%)
RESN	73.8 ± 1.14[b]	0.16 ± 0.01[b]	96.3	99.5
RES	11172.9 ± 3120	1.11 ± 0.19		

[a]Abbreviations: RESN, resveratrol nanoparticle system; RES, resveratrol. [b]$P < 0.05$.

Encapsulation Efficiency of RESN. The determination of encapsulation efficiency and yield is the best method to evaluate the amount of active compound successfully encapsulated in a pharmaceutical formulation. As Table 1 shows, the encapsulation efficiency and yield of RESN were 99.5% and 96.3%, respectively. This result indicates that a ratio of RES:EE100:PVA (1:4:4) effectively encapsulated RES into a nanoparticle formulation using the nanoparticle engineering process. By contrast, the low ratio of RES:EE100:PVA (1:1:1) achieved less than 5% encapsulation efficiency and yield (data not shown). Jyothi et al. have also reported that the concentration of the excipients is the major factor influencing encapsulation efficiency of pharmaceutical formulations.[24]

Crystalline Transform to Amorphous. It is important that the crystalline form of an active compound be transformed to an amorphous state with excipients to enhance the dissolution percentage. Previous studies have demonstrated that differential scanning calorimetry is one useful tool to characterize the thermal behavior of compounds and is also used to elucidate the crystalline transformation between active compound and excipients; examples include quercetin and kaempferol.[20,25] The DSC thermograms (Figure 1A) show that a sharp endothermic peak of RES was obtained at 268.5 °C, corresponding to the melting point. After application of the nanoparticle engineering process, no melting point peak was observed in the case of RESN, which implies a crystalline transformation between RES and excipients, suggesting a molecular dispersion of RES into the EE100/PVA. Furthermore, the physical mixture (RESPM, RES:EE100:PVA, 1:4:4) did not exhibit the melting point peak. We also used a low ratio (RES:EE100:PVA, 1:1:1) to confirm the observation, and obtained the same result with high ratio (data not shown). The glass transition temperature of EE100 as obtained from a pharmaceutical manufacturer is near 48 °C, and we suggest that EE100 could be fused with RES during the heating procedure. Similar results were obtained by Tzeng et al.[25]

Additionally, we used XRD to confirm the crystalline transformation of RES and its nanoparticle formulation (Figure 1B). Diffraction angles (2θ) of 6.6°, 13.2°, 16.4°, 19.2°, 22.3°, 23.6°, and 28.3° were displayed in the XRD pattern of RES, clearly indicating the crystalline structure of RES. The characteristic peaks of RES in the analysis of RESPM were diminished, but the crystalline structure of RES was still retained. Importantly, all characteristic peaks of RES were not found in the XRD pattern of RESN. These results indicated that the nanoparticle engineering process effectively encapsulated RES into EE100/PVA, thus rendering the clustered crystalline structure amorphous, an effect not achieved by a general mixing method. Similar findings were observed in quercetin nanoparticles and triclosan nanoparticles.[20,26]

Hydrogen-Bond Formation between Drug and Excipients. The present study used FT-IR and ^{1}H NMR to elucidate the intermolecular interaction between RES and EE100/PVA. The FT-IR spectrum of RES (Figure 2A) showed that there is an OH stretching signal at 3270 cm^{-1} that is also seen in RESPM, indicating there is no intermolecular interaction between RES and EE/PVA during physical mixing. However, the FT-IR spectrum of RESN showed that the OH stretching was shifted to 3389 cm^{-1}, indicating that an intermolecular hydrogen-bonding interaction occurred between RES and EE100/PVA. In addition, a comparison of ^{1}H NMR spectra of RES and RESN is shown in Figure 2B. The spectrum of RES showed that protons on the aromatic group appear from 6 to 8 ppm, and the protons on the hydroxyl group were at 9.25 ppm (C3-OH and C5-OH) and 9.59 ppm (C4′-OH). However, a hydroxyl group signal disappeared in the spectrum of RESN, indicating that an intermolecular hydrogen-bonding interaction

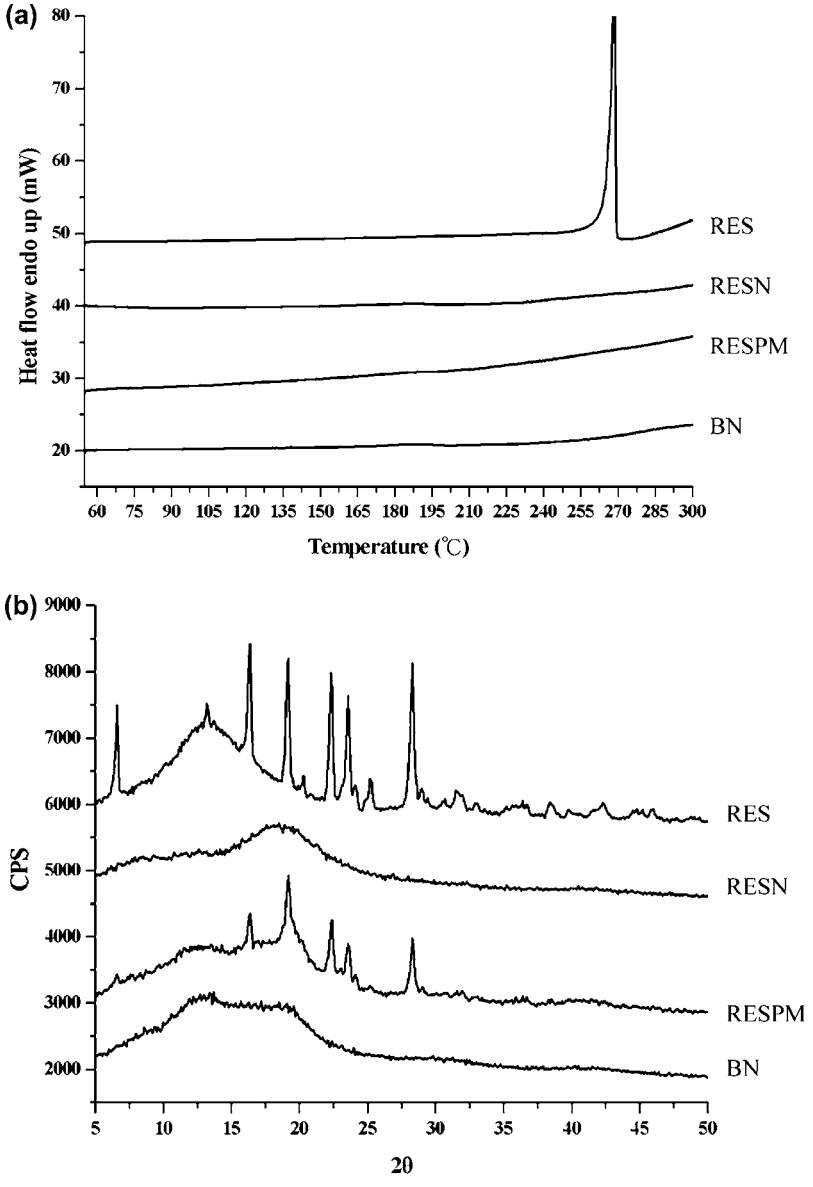

Figure 1. The crystalline active compound was transformed to an amorphous state with excipients. DSC (A) and XRD (B) patterns of RES, RESN, RESPM, and BN.

formed between RES and EE100/PVA. A similar result was observed by Horisawa et al., who showed that the tertiary amine of EE100 formed an intermolecular hydrogen bond with a poorly water-soluble anti-inflammatory drug.[27]

Dissolution Profile of RES and RESN. The dissolution profiles of raw RES and its nanoparticle in pH 1.2 and 4.5 buffer solutions are shown in Figure 3. The dissolution percentage of raw RES was respectively 40% and 55% in pH 1.2 and 4.5 within 120 min. The dissolution percentage of the drug from the RESN showed that more RES dissolved in pH 1.2 (51%) and 4.5 (75%) within 120 min. In comparison, it was evident that RESN quickly released more than 55% after 10 min and finally released 75% within 120 min under pH 4.5. Thus, the dissolution percentage of RESN from the nanoparticle system was increased by 20% compared with free RES.

Hepatoprotective Effect of RES and RESN as Shown by Liver Function Markers and Histopathological Observation. Figure 4 shows liver function markers in the control, pretreatment with vehicle (nanoparticle without RES), RES, and RESN groups. The AST (Figure 4A) and ALT (Figure 4B) levels in the vehicle and CCl_4-induced group were significantly increased compared to the vehicle group ($P < 0.05$). RESN (20 mg) significantly lowered the AST and ALT levels in rats subjected to CCl_4-induced hepatotoxicity compared to vehicle group ($P < 0.05$). RES treatment lowered the ALT and AST levels, but not significantly. On the other hand, the results of histopathological observation on the liver tissues after various groups are shown in Figure 4. There was regular cellular architecture with central vein and no necrosis, inflammation, nor vascular degeneration in the vehicle group (Figure 4C). In contrast with vehicle group, the liver section of CCl_4-intoxicated group presented destructive hepatic cell necrosis, including ballooning degeneration and fatty change (Figure 4D). In addition, RES treatment could reduce the CCl_4-induced liver injury, but some hepatocytes still had ballooning degeneration and fatty change (Figure 4E). RESN treatment more effectively ameliorated the hepatic cell damage and inflammation after CCl_4 intoxication (Figure 4F). There-

dx.doi.org/10.1021/jf2050137 | J. Agric. Food Chem. 2012, 60, 4662–4671

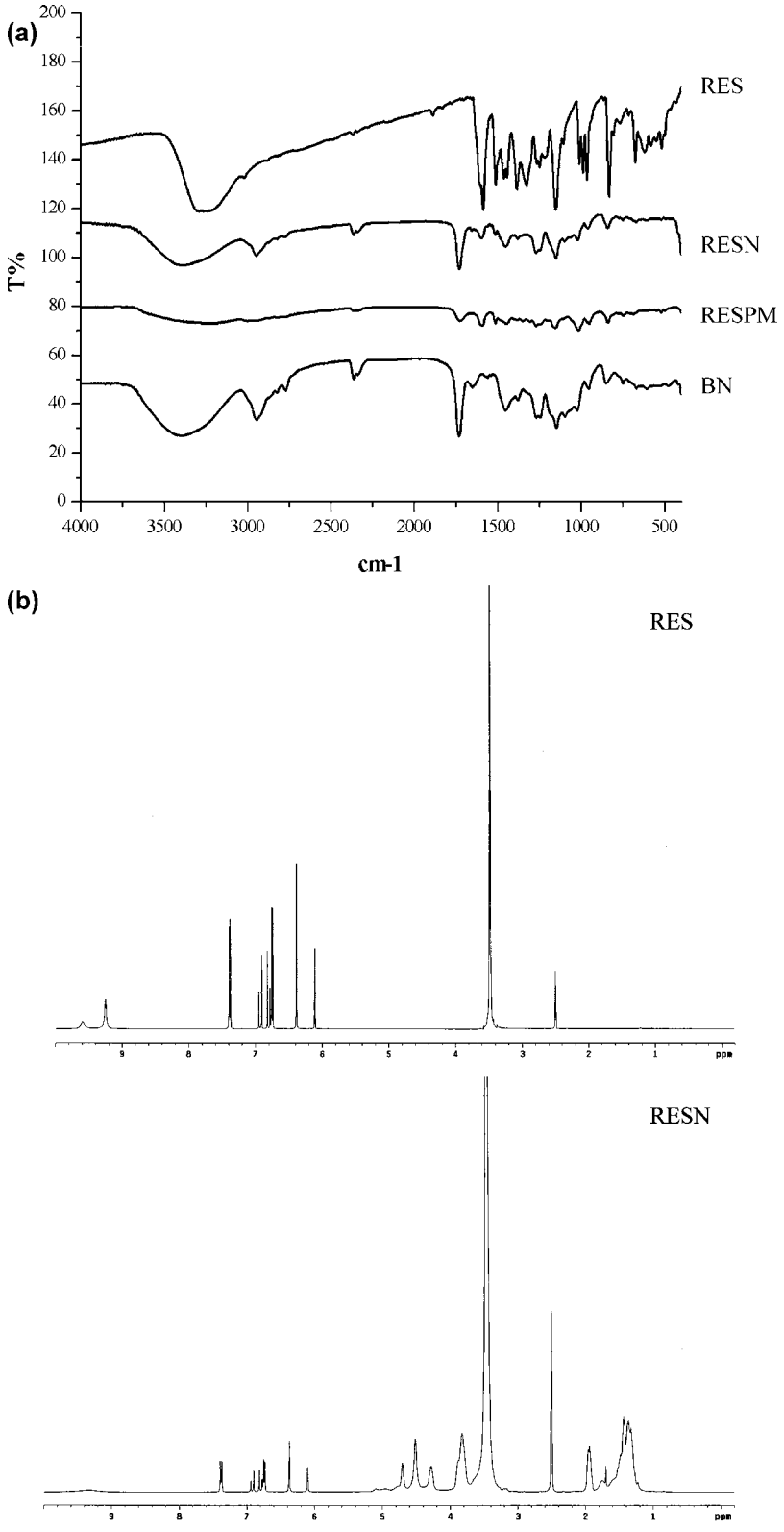

Figure 2. Hydrogen-bond formation between drug and excipients. FT-IR pattern (A) of RES, RESN, RESPM, and BN. ^{1}H NMR spectra (B) of RES and RESN.

fore, RESN exerts a better hepatoprotective effect than RES, as indicated by liver function markers and histopathological observation.

ROS Content and Lipid Peroxidation of Liver Tissue. Figure 5 shows that the vehicle-treated CCl_4-induced group exhibited significantly increased ROS content and lipid peroxidation compared to the vehicle group ($P < 0.05$). Pretreatment with RES and RESN significantly lowered the lipid peroxidation of liver tissue ($P < 0.05$). Additionally, RESN treatment significantly reduced the ROS content of liver tissue,

dx.doi.org/10.1021/jf2050137 | J. Agric. Food Chem. 2012, 60, 4662–4671

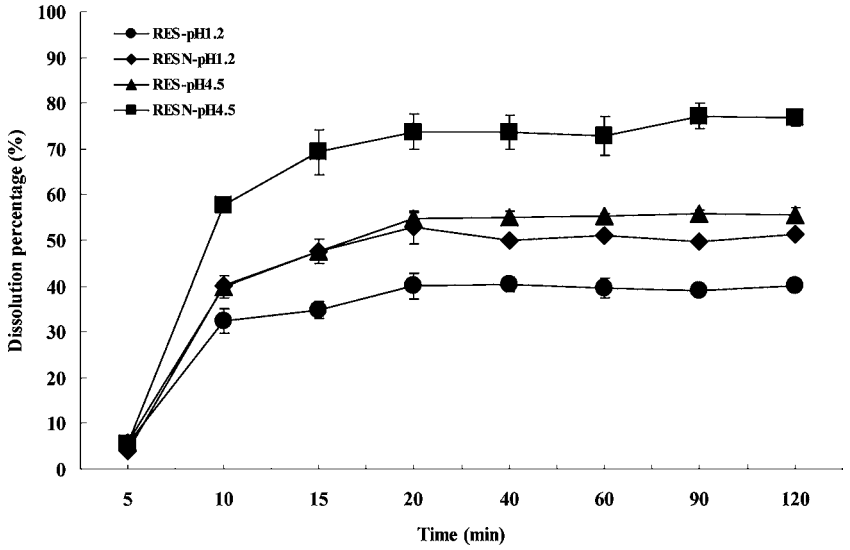

Figure 3. The profiles of dissolution percentage of RES and RESN under pH 1.2 and pH 4.5. Values are expressed as mean ± SD, $n = 6$.

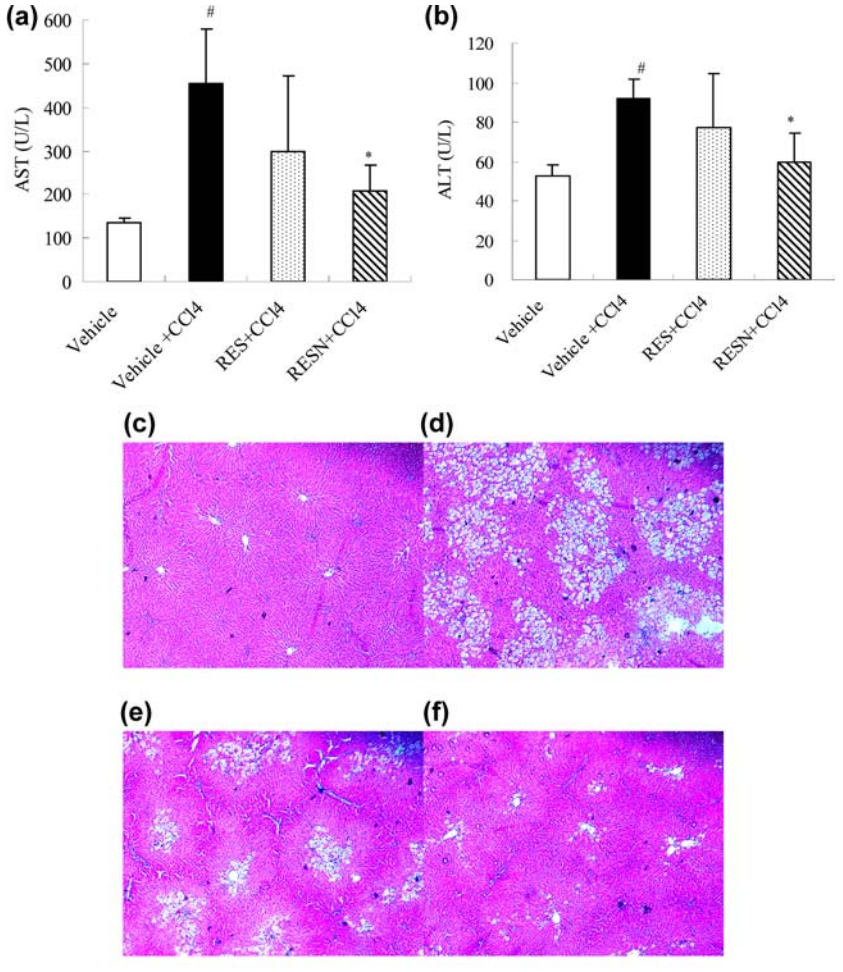

Figure 4. The levels of liver function markers from RES and RESN in CCl_4-induced hepatotoxicity in rats: AST (A) and ALT (B). Values are expressed as mean ± SD, $n = 5$. $^{\#}P < 0.05$ vs vehicle group. $^{*}P < 0.05$ vs vehicle with CCl_4-induced group. In addition, the histopathological observation of the liver tissues after various treatments: vehicle (C), CCl_4 with vehicle (D), CCl_4 with RES (E), and CCl_4 with RESN (F).

but RES had no effect, indicating that RESN exerts better antioxidant activity than RES.

Inflammatory Cytokines Expression. TNF-α and IL-1β have been reported to play an important role in the inflammation seen with CCl_4-induced hepatoxicity.[28] As Figure 6 shows, increased TNF-α and IL-1β levels in serum were observed in rats with CCl_4-induced hepatotoxicity compared with the control group ($P < 0.05$). The CCl_4-induced group

dx.doi.org/10.1021/jf2050137 | J. Agric. Food Chem. 2012, 60, 4662–4671

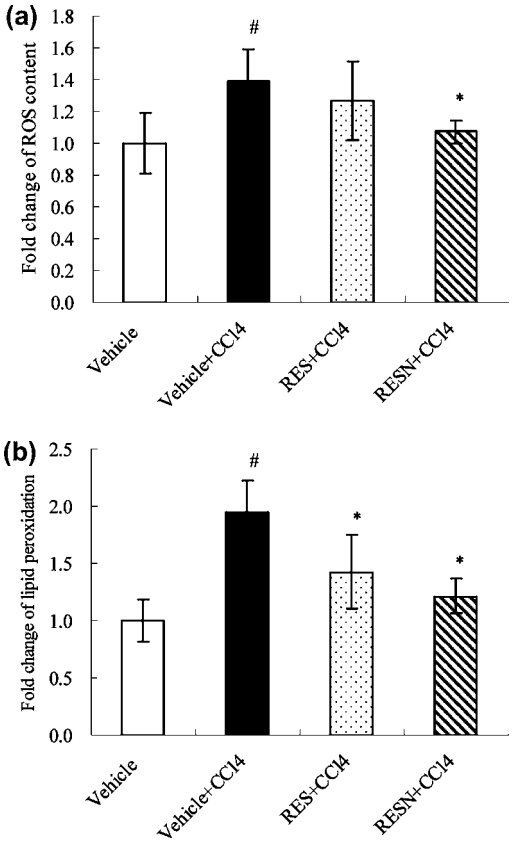

Figure 5. The index of oxidative stress of liver tissue in CCl_4-induced hepatotoxicity in rats: ROS content (A) and lipid peroxidation (B). Values are expressed as mean ± SD, $n = 5$. $^{\#}P < 0.05$ vs vehicle group. $^{*}P < 0.05$ vs vehicle with CCl_4-induced group.

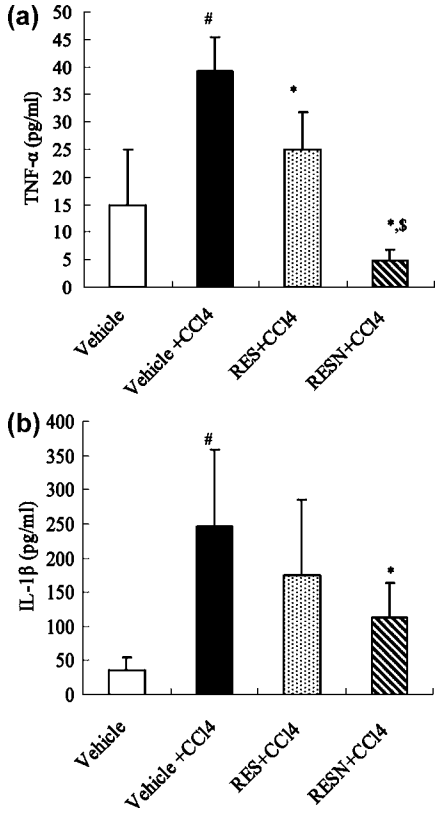

Figure 6. The inflammatory cytokines of serum on CCl_4-induced hepatotoxicity in rats: TNF-α (A) and IL-1β (B). Values are expressed as mean ± SD, $n = 5$. $^{\#}P < 0.05$ vs vehicle group. $^{*}P < 0.05$ vs vehicle with CCl_4-induced group. $^{\$}P < 0.05$ compared to RES.

pretreated with RES and RESN showed a significant reduction in the activation of TNF-α ($P < 0.05$), and RESN had a stronger effect on TNF-α levels as compared with RES. RESN, but not RES, significantly lowered IL-1β levels ($P < 0.05$). Moreover, Figure 7 shows that the protein levels of COX-2, cPLA2, iNOS, and caspase-3 were increased by approximately 2.0-, 1.4-, 2.2-, and 1.2-fold, respectively, compared to the control group ($P < 0.05$). In the treatment group with RES and RESN, expression levels of COX-2, cPLA2, and iNOS were markedly reduced to near normal levels ($P < 0.05$). RESN, but not RES, exerted a significant effect on caspase-3. Additionally, RESN significantly reduced the level of COX-2 as compared with RES ($P < 0.05$).

DISCUSSION

Drug delivery systems (DDS) have been widely used to overcome the poor water solubility of compounds and enhance their dissolution percentage by improving their physicochemical properties. NPS is a DDS that possesses several advantages, including simple and rapid preparation and good reproducibility.[18] The present study has demonstrated that EE100/PVA successfully encapsulated RES by a simple NPS technique and improved the physicochemical properties of RES for enhancing dissolution percentage, including particle size reduction, amorphous transformation, and hydrogen bonding with excipients. According to the Noyes and Whitney equation, particle size reduction is frequently the first choice for improving the dissolution percentage of poorly water-soluble compounds in pharmaceutical, food, and cosmetic science.[29] Previous studies have demonstrated that particle size reduction effectively increased the surface area of compounds and therefore enhanced the dissolution percentage.[30,31] Our results showed that the particle size of RESN is smaller than that of RES, leading to increased surface area and enhanced dissolution percentage.

In addition, the crystal-to-amorphous change between compounds and excipients has been shown to enhance the dissolution percentage of compounds. Our findings demonstrated that RES was dispersed into the EE100/PVA, and the clustered crystalline structure was changed to an amorphous structure by intermolecular interactions with the excipients. Many studies have demonstrated that intermolecular interaction between poorly water-soluble compounds and excipients effectively improved the dissolution percentage.[32,33] Our data demonstrated that the aromatic ring of RES effectively formed an intermolecular hydrogen bond with the EE100 and PVA that is used as an emulsion stabilizer to form stable nanoparticle systems. Horisawa et al. have also demonstrated that the tertiary amine of EE100 could form an intermolecular hydrogen bond with a poorly water-soluble anti-inflammatory drug.[27] Finally, the dissolution percentage of RES from the nanoparticles system was 25% higher compared with free RES, due to the improvement of the physicochemical properties of RES.

RES is a good antioxidant that could function to maintain the health of the body during excessive oxidative stress; however, pharmaceutical preparation of RES might influence its antioxidant activity. To address this question, we performed a hepatotoxicity animal study to compare the hepatoprotective activity of RES and RESN. CCl_4 is a well-known toxicant

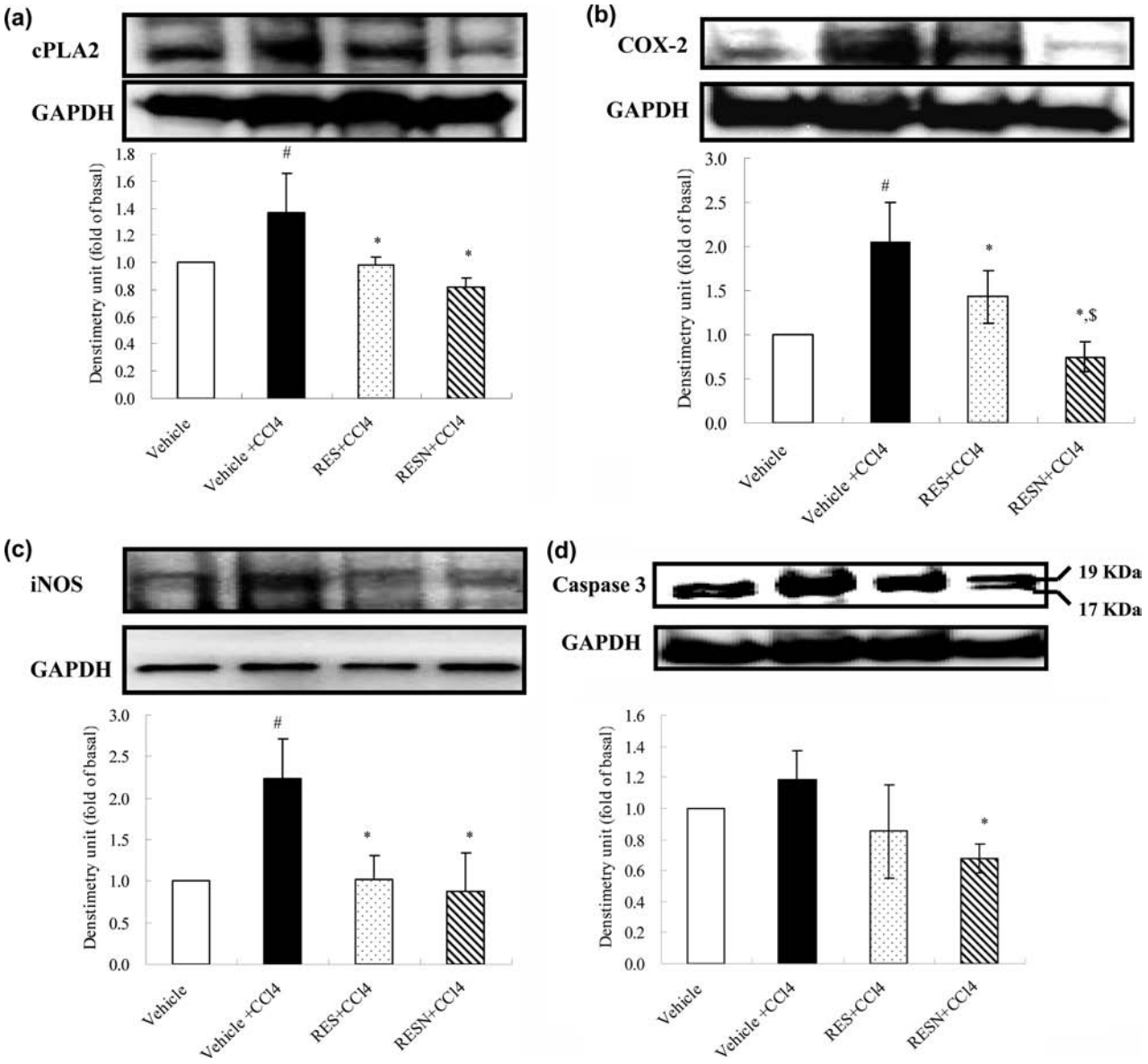

Figure 7. Inflammatory protein expression of liver tissue on CCl_4-induced hepatotoxicity in rats: cPLA2 (A), COX-2 (B), iNOS (C), and caspase-3 (D). All determinations were performed in triplicate. $^{\#}P < 0.05$ vs vehicle group. $^{*}P < 0.05$ vs vehicle with CCl_4-induced group. $^{\$}P < 0.05$ between RES.

commonly used to induce hepatotoxicity for evaluating hepatoprotective activity in rats. During CCl_4 intoxication, liver function markers (ALT and AST) leak into the blood, reflecting hepatocyte death.[34] Our data demonstrated that pretreatment with RESN decreased the leakage of AST and ALT from injured hepatocytes and prevented the progression of CCl_4-induced hepatotoxicity more effectively than RES. Hepatocyte death due to CCl_4 intoxication is believed to involve two major pathways: oxidative stress and inflammation. Hence, we investigated the antioxidant and anti-inflammatory effects of RES and RESN during CCl_4 intoxication to elucidate the hepatoprotective mechanisms.

Many hepatoprotective compounds, such as berberine and curcumin, prevent CCl_4-induced hepatotoxicity by antioxidant mechanisms.[35,36] It is well-known that CCl_4 is metabolized and catalyzed by a microsomal cytochrome P450-dependent monooxygenase system in liver and other organs. CCl_4 is first metabolized to trichloromethyl free radical ($^{\bullet}CCl_3$), which reacts very rapidly with oxygen and forms another toxic free radical, trichloromethyl peroxy radical ($^{\bullet}CCl_3{}^{\bullet}OO^{\bullet}$).[37] At the same time, ROS are rapidly overproduced in rats with CCl_4-induced hepatotoxicity. These ROS, such as superoxide anion, hydrogen peroxide, and hydroxyl radical, then initiate the peroxidation of unsaturated fatty acids of phospholipids and protein in the hepatocyte membrane, leading to hepatocyte death. Antioxidant enzymes of hepatocytes, including superoxide dismutase and glutathione peroxidase, are apparently depleted by ROS and lipid peroxide overproduction.[34,38] Our study demonstrated that ROS overproduction and lipid peroxidation are the oxidative stresses that cause hepatocyte death in rats with CCl_4-induced hepatotoxicity. Our data showed that pretreatment with RESN and RES effectively decreased the amount of ROS, lowered the lipid peroxidation in the hepatocyte membrane, and also reduced the leakage of AST and ALT from dying hepatocytes to prevent the CCl_4-intoxication-mediated progression of hepatotoxicity. We

dx.doi.org/10.1021/jf2050137 | J. Agric. Food Chem. 2012, 60, 4662–4671

suggest that RESN and RES play a hepatoprotective role by reducing oxidative stress.

In addition, an effect of the anti-inflammation pathway on hepatoprotective mechanisms has been shown during CCl_4-induced acute hepatotoxicity. CCl_4 and its metabolite rapidly activate Kupffer cells and macrophages to overproduce pro-inflammatory cytokines such as TNF-α and IL-1β.[39] Excessive production of pro-inflammatory cytokines elicits a phagocytic oxidative metabolism reaction mediated by iNOS, leading to overproduction of nitric oxide and further severe inflammatory injury during CCl_4-induced acute hepatotoxicity. Moreover, previous studies have shown that phospholipase A2 family members are important in several cellular signaling processes and are known to play a significant inflammatory role in CCl_4-induced hepatocyte injury. CCl_4 may increase the cytosolic calcium concentration to activate the cPLA2. This enzyme metabolizes phospholipids to arachidonic acid and a lysophospholipid, immediately causing membrane lipid peroxidation, leading to cell death.[40,41] Additionally, TNF-α promotes apoptosis through binding to TNF-receptor 1 leading to activation of caspase-3. Caspase-3 can cleave and inactivate plasma membrane calcium transport systems to induce hepatocyte membrane lysis and secondary necrosis such as in CCl_4-induced acute hepatotoxicity. In turn, cPLA2 is further activated by caspase-3 and activated downstream caspases, resulting in arachidonic acid overproduction and hepatocyte apoptosis.[41,42] Our data indicate that CCl_4 participates in the activation of caspase-3 and cPLA2 to induce apoptosis of hepatocytes. Consequently, by reducing production of these initial pro-inflammatory cytokines in the chain reaction of inflammation, RESN and RES were able to decrease COX-2, iNOS, cPLA2, and caspase-3 levels and thereby prevent hepatocyte apoptosis induced by overproduction of TNF-α and IL-1β. We suggest that RESN and RES play another role in the hepatoprotective mechanism by preventing inflammatory responses.

In our comparative analysis of the hepatoprotective effects of RES and RESN, RESN displayed significantly greater antioxidant and anti-inflammatory activities on CCl_4-induced acute hepatotoxictiy in rats. Roerdink et al. have indicated that liposomes and polymeric nanospheres (in the size range of 50−200 nm) are effectively extravasated into hepatic parenchymal and increased capillary permeability.[43] In addition, Drummond et al. have also been discussed that doxorubicin-loaded PEG liposome (in the size range of 70−200 nm) had better anticancer activity when compared with raw doxorubicin.[44] Therefore, it is important to note that liver injury leads to macrophage activation in the bloodstream and macrophage invasion of the liver; in turn, macrophages can efficiently take up and deliver the nanoparticle drug into inflamed liver tissue, leading to accumulation of the nanoparticle drug in the liver.[45] The particle size of RESN was less than 100 nm and RESN had better dissolution properties than RES, suggesting that a higher concentration of bioactive ingredient could be taken up and delivered into the bloodstream and injured liver tissue. However, the present study suggested that RESN exceeded RES in hepatoprotective effect by reducing particle size and enhancing dissolution percentage.

In conclusion, the present study shows effective development of a novel RES nanoparticle delivery system and the enhancement of dissolution properties of RES by reducing particle size and improving physicochemical characteristics, which are crucial factors for achieving optimal in vivo efficacy. The animal model of CCl_4-induced hepatotoxicity established the superiority of RESN over RES in hepatoprotective effect, likely due to its better antioxidant and anti-inflammatory activities. Consequently, we suggest that RESN deserves further study and may be useful in prophylaxis of chronic liver diseases.

AUTHOR INFORMATION

Corresponding Author

*C.-C.L.: tel, +886-7-3121101, ext. 2122; fax, +886-7-3135215; e-mail, aalin@kmu.edu.tw. W.-S.T.: tel, +886-6-2812811, ext. 53130; e-mail, tws.ws4664@msa.hinet.net.

Funding

The work was supported by grants from the Chi-Mei Medical Center and the Kaohsiung Medical University Research Foundation (99CM-KMU-06), National Science Council of Taiwan (NSC 99-2313-B-255-001-MY3) and Chang Gung Medical Research Program Foundation (CMRPF6A0081).

Notes

The authors declare no competing financial interest.

REFERENCES

(1) Jaeschke, H. Reactive oxygen and mechanisms of inflammatory liver injury: Present concepts. *J. Gastroenterol. Hepatol.* **2011**, *Suppl 1*, 173−179.

(2) Ferre, N.; Claria, J. New insights into the regulation of liver inflammation and oxidative stress. *Mini Rev. Med. Chem.* **2006**, *6*, 1321−1330.

(3) Obrenovich, M. E.; Nair, N. G.; Beyaz, A.; Aliev, G.; Reddy, V. P. The role of polyphenolic antioxidants in health, disease, and aging. *Rejuvenation Res.* **2010**, *13*, 631−643.

(4) Rodrigo, R.; Miranda, A.; Vergara, L. Modulation of endogenous antioxidant system by wine polyphenols in human disease. *Clin. Chim. Acta* **2011**, *12*, 410−424.

(5) Lippi, G; Franchini, M; Favaloro, E. J.; Targher, G. Moderate red wine consumption and cardiovascular disease risk: Beyond the "French paradox". *Semin. Thromb. Hemost.* **2010**, *36*, 59−70.

(6) Standridge, J. B.; Zylstra, R. G.; Adams, S. M. Alcohol consumption: An overview of benefits and risks. *South. Med. J.* **2004**, *97*, 664−672.

(7) Bujanda, L. The effects of alcohol consumption upon the gastrointestinal tract. *Am. J. Gastroenterol.* **2000**, *95*, 3374−3382.

(8) Lyons, M. M.; Yu, C.; Toma, R. B. Resveratrol in raw and baked blueberries and bilberries. *J. Agric. Food Chem.* **2003**, *51*, 5867−5870.

(9) de la Lastra, C. A.; Villegas, I. Resveratrol as an antioxidant and pro-oxidant agent: Mechanisms and clinical implications. *Biochem. Soc. Trans.* **2007**, *35*, 1156−1160.

(10) Zhang, F.; Liu, J.; Shi, J. S. Anti-inflammatory activities of resveratrol in the brain: Role of resveratrol in microglial activation. *Eur. J. Pharmacol.* **2010**, *636*, 1−7.

(11) Shukla, Y.; Singh., R. Resveratrol and cellular mechanisms of cancer prevention. *Ann. N. Y. Acad. Sci.* **2011**, *1215*, 1−8.

(12) Albani, D.; Polito, L.; Signorini, A.; Forloni, G. Neuroprotective properties of resveratrol in different neurodegenerative disorders. *Biofactors* **2010**, *36*, 370−376.

(13) Das, M.; Das, D. K. Resveratrol and cardiovascular health. *Mol. Aspects Med.* **2010**, *31*, 503−512.

(14) Bishayee, A.; Darvesh, A. S.; Politis, T.; McGory, R. Resveratrol and liver disease: From bench to bedside and community. *Liver Int.* **2010**, *30*, 1103−1114.

(15) Baur, J. A.; Sinclair, D. A. Therapeutic potential of resveratrol: The in vivo evidence. *Natl. Rev. Drug Discovery* **2006**, *5*, 493−506.

(16) Ratnam, D. V.; Ankola, D. D.; Bhardwaj, V.; Sahana, D. K.; Kumar, M. N. Role of antioxidants in prophylaxis and therapy: A pharmaceutical perspective. *J. Controlled Release* **2006**, *113*, 189−207.

(17) Mallick, S.; Pattnaik, S.; Swain, K.; De, P. K. Current perspectives of solubilization: Potential for improved bioavailability. *Drug Dev. Ind. Pharm.* **2007**, *33*, 865−873.
(18) Hu, J.; Johnston, K. P.; Williams, R. O., 3rd. Nanoparticle engineering processes for enhancing the dissolution rates of poorly water soluble drugs. *Drug Dev. Ind. Pharm.* **2004**, *30*, 233−245.
(19) Bilati, U.; Allemann, E.; Doelker, E. Development of a nanoprecipitation method intended for the entrapment of hydrophilic drugs into nanoparticles. *Eur. J. Pharm. Sci.* **2005**, *24*, 67−75.
(20) Wu, T. H.; Yen, F. L.; Lin, L. T.; Tsai, T. R.; Lin, C. C.; Cham, T. M. Preparation, physicochemical characterization, and antioxidant effects of quercetin nanoparticles. *Int. J. Pharm.* **2008**, *346*, 160−168.
(21) Ikeda, H.; Kume, Y.; Tejima, K.; Tomiya, T.; Nishikawa, T.; Watanabe, N.; Ohtomo, N.; Arai, M.; Arai, C.; Omata, M.; Fujiwara, K.; Yatomi, Y. Rho-kinase inhibitor prevents hepatocyte damage in acute liver injury induced by carbon tetrachloride in rats. *Am. J. Physiol. Gastrointest. Liver Physiol.* **2007**, *293*, 911−917.
(22) Llacuna, L.; Mari, M.; Lluis, J. M.; Garcia-Ruiz, C.; Fernandez-Checa, J. C.; Morales, A. Reactive oxygen species mediate liver injury through parenchymal nuclear factor-kappaB inactivation in prolonged ischemia/reperfusion. *Am. J. Pathol.* **2009**, *174*, 1776−1785.
(23) Ohkawa, H.; Ohishi, N.; Yagi, K. Assay for lipid peroxides in animal tissues by thiobarbituric acid reaction. *Anal. Biochem.* **1979**, *95*, 351−358.
(24) Jyothi, N. V.; Prasanna, P. M.; Sakarkar, S. N.; Prabha, K. S.; Ramaiah, P. S.; Srawan, G. Y. Microencapsulation techniques, factors influencing encapsulation efficiency. *J. Microencapsul.* **2010**, *27*, 187−197.
(25) Tzeng, C. W.; Yen, F. L.; Wu, T. H.; Ko, H. H.; Lee, C. W.; Tzeng, W. S.; Lin, C. C. Enhancement of dissolution and antioxidant activity of kaempferol using a nanoparticle engineering process. *J. Agric. Food Chem.* **2011**, *59*, 5073−5080.
(26) Piñón-Segundo, E.; Ganem-Quintanar, A.; Alonso-Perez, V.; Quintanar-Guerrero, D. Preparation and characterization of triclosan nanoparticles for periodontal treatment. *Int. J. Pharm.* **2005**, *294*, 217−232.
(27) Horisawa, E.; Danjo, K.; Haruna, M. Physical properties of solid dispersion of a nonsteroidal anti-inflammatory drug (M-5011) with Eudragit E. *Drug Dev. Ind. Pharm.* **2000**, *26*, 1271−1278.
(28) Choi, J. H.; Kim, D. W.; Yun, N.; Choi, J. S.; Islam, M. N.; Kim, Y. S.; Lee, S. M. Protective effects of hyperoside against carbon tetrachloride-induced liver damage in mice. *J. Nat. Prod.* **2011**, *74*, 1055−1060.
(29) Dokoumetzidis, A.; Macheras, P. A century of dissolution research: From Noyes and Whitney to the biopharmaceutics classification system. *Int. J. Pharm.* **2006**, *321*, 1−11.
(30) Xia, D.; Cui, F.; Piao, H.; Cun, D.; Piao, H.; Jiang, Y.; Ouyang, M.; Quan, P. Effect of crystal size on the in vitro dissolution and oral absorption of nitrendipine in rats. *Pharm. Res.* **2010**, *27*, 1965−1976.
(31) Kamiya, S.; Kurita, T.; Miyagishima, A.; Itai, S.; Arakawa, M. Physical properties of griseofulvin-lipid nanoparticles in suspension and their novel interaction mechanism with saccharide during freeze-drying. *Eur. J. Pharm. Biopharm.* **2010**, *74*, 461−466.
(32) Andrews, G. P.; AbuDiak, O. A.; Jones, D. S. Physicochemical characterization of hot melt extruded bicalutamide−polyvinylpyrrolidone solid dispersions. *J. Pharm. Sci.* **2010**, *99*, 1322−1335.
(33) Li, B.; Wen, M.; Li, W.; He, M.; Yang, X.; Li, S. Preparation and characterization of baicalin−polyvinylpyrrolidone coprecipitate. *Int. J. Pharm.* **2011**, *408*, 91−96.
(34) Weber, L. W.; Boll, M.; Stampfl, A. Hepatotoxicity and mechanism of action of haloalkanes: Carbon tetrachloride as a toxicological model. *Crit. Rev. Toxicol.* **2003**, *33*, 105−136.
(35) Domitrović, R.; Jakovac, H.; Blagojević, G. Hepatoprotective activity of berberine is mediated by inhibition of TNF-alpha, COX-2, and iNOS expression in CCl_4-intoxicated mice. *Toxicology* **2011**, *280*, 33−43.
(36) Kamalakkannan, N.; Rukkumani, R.; Varma, P. S.; Viswanathan, P.; Rajasekharan, K. N.; Menon, V. P. Comparative effects of curcumin and an analogue of curcumin in carbon tetrachloride-induced hepatotoxicity in rats. *Basic Clin. Pharmacol. Toxicol.* **2005**, *97*, 15−21.
(37) Koop, D. R. Oxidative and reductive metabolism by cytochrome P450 2E1. *FASEB J.* **1992**, *6*, 724−730.
(38) Basu, S. Carbon tetrachloride-induced lipid peroxidation: Eicosanoid formation and their regulation by antioxidant nutrients. *Toxicology* **2003**, *189*, 113−127.
(39) Luster, M. I.; Simeonova, P. P.; Gallucci, R. M.; Bruccoleri, A.; Blazka, M. E.; Yucesoy, B. Role of inflammation in chemical-induced hepatotoxicity. *Toxicol. Lett.* **2001**, *120*, 317−321.
(40) Basu, S. Novel cyclooxygenase-catalyzed bioactive prostaglandin F2 alpha from physiology to new principles in inflammation. *Med. Res. Rev.* **2007**, *27*, 435−468.
(41) Cummings, B. S.; McHowat, J.; Schnellmann, R. G. Phospholipase A2s in cell injury and death. *J. Pharmacol. Exp. Ther.* **2000**, *294*, 793−799.
(42) Bhave, V. S.; Donthamsetty, S.; Latendresse, J. R.; Mehendale, H. M. Inhibition of cyclooxygenase-2 aggravates secretory phospholipase A2-mediated progression of acute liver injury. *Toxicol. Appl. Pharmacol.* **2008**, *228*, 239−246.
(43) Roerdink, F.; Regts, J.; Van Leeuwen, B.; Scherphof, G. Intrahepatic uptake and processing of intravenously injected small unilamellar phospholipid vesicles in rats. *Biochim. Biophys. Acta* **1984**, *770*, 195−202.
(44) Drummond, D. C.; Meyer, O.; Hong, K.; Kirpotin, D. B.; Papahadjopoulos, D. Optimizing liposomes for delivery of chemotherapeutic agents to solid tumors. *Pharmacol. Rev.* **1999**, *51*, 691−743.
(45) Moghimi, S. M.; Hunter, A. C.; Murray, J. C. Long-circulating and target-specific nanoparticles: Theory to practice. *Pharmacol. Rev.* **2001**, *53*, 283−318.